Scalability of Silicon Photonic Microring Based Switch

Dessislava Nikolova, Robert Hendry, Sébastien Rumley and Keren Bergman
Department of Electrical Engineering, Columbia University, 500 W. 120th St., New York, NY 10027, USA
e-mail: dnn2108@columbia.edu

ABSTRACT
High radix switches are essential for reducing network latency. A possible way to realize them is by using silicon photonic microrings which have been demonstrated to have small foot prints and very fast switching times. By cascading multiple 2 by 2 switches high radix ones can be achieved. However, the scalability of such microring-resonator based switch fabrics is limited by optical power loss and crosstalk. In this work we employ detailed physical layer device models to determine the scalability of such switches. Our results show that a high radix switch with low cross talk and insertion loss is feasible.
Keywords: Optical switching, silicon photonics, cross talk, high radix switch.

1. INTRODUCTION

Silicon photonics is a promising medium for optical transmission due to its dense wavelength-division-multiplexing (WDM) capabilities, as well as its low power and small area footprint devices. Ongoing research is continually improving silicon photonic devices and expanding the functionality of this technology. Microring resonators, in particular, have been demonstrated to be able to implement wide variety of functions necessary for optical transmission systems, including optical switching, signal modulation, and filtering. Moreover, silicon photonic microrings are capable of switching multiple wavelengths simultaneously [1-3], enabling very high bandwidth all-optical networks. Higher radix switches can be achieved by cascading multiple such ring-based switches [4,5]. But, deleterious effects from these devices, in particular insertion loss and cross talk, can have a very significant impact on the transiting optical signal qualities. They limit the scalability of all-optical communication paths, and therefore the performance we can expect from silicon photonic networks. Consequently, these effects must be carefully estimated and, if possible, minimized.

As high radix transparent switches are deemed more effective in reducing interconnect sizes [6,7], one is interested in maximizing this figure. Prior studies have been conducted to estimate the maximal scalability of ring based switches, considering different cascading architectures [8,9]. However, to the best of our knowledge, analyses conducted so far model the deleterious effects of the switches based on extrapolations from lab-measurements of single devices. They do not capture the real dependence of the switch scalability on wavelength channel spacing, controllable device coupling, and other physical parameters. To fully capture these aspects, low-level modelling, such as finite element method simulations, could offer very precise predictions. However, due to the very long time they take to calculate large optical networks, they are reserved for single device design.

In this work, we present a physical layer model able to capture the important device parameters while staying computationally tractable. Based on the transfer matrix method from [10,11], it lets us analyse the scalability of microring resonator based switch fabrics. We show that, in order to reach the theoretical limits of performance, the physical parameters must be optimized depending on the layout of the fabric. Once the optimal set of parameters is identified, more rigorous electromagnetic field modelling techniques can be used to design a device matching this set. Furthermore we illustrate how our physical model can be leveraged to predict the performance of silicon photonic networks in terms of link bandwidth and aggregate fabric capacity.

2. SILICON PHOTONIC MICRORING SWITCH

Our analysis starts by considering a basic switching element, schematically drawn on figure 1 a), which consists of two silicon microring resonators coupled to two silicon waveguides at their crossing. When the rings are on resonance with an input signal, this signal is coupled to the ring and "dropped" onto the other waveguide as shown on figure 1a). When the rings are off resonance, the signal passes through the switch remaining on the same waveguide as shown on figure 1 b). Both inputs can be dropped into or allowed to pass by the rings simultaneously which allows this type of switch to be used in composing non-blocking networks. However, when two signals are present in the switch intrachannel crosstalk occurs. To become controllable, the resonators are realized as p-n junctions. Application of an electrical signal allows the injection of carriers into the ring, affecting the refractive index through free-plasma dispersion, and changing its resonant frequencies. The size of the rings determines the periodicity of the resonances

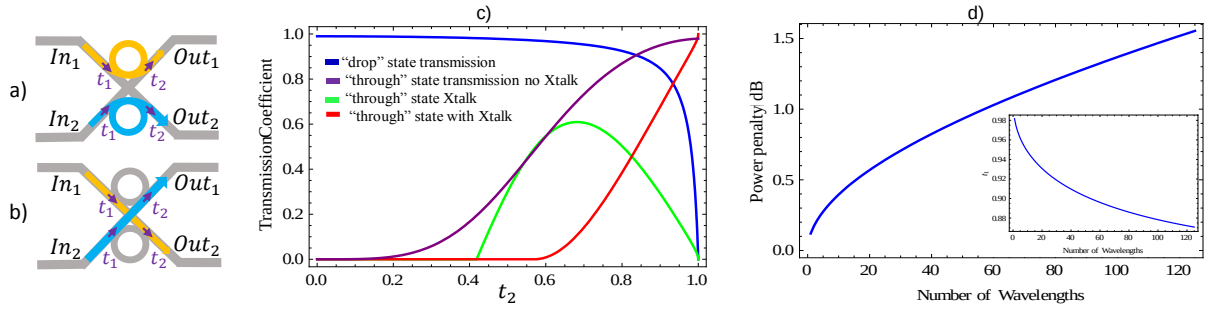

Figure 1. Switch element in a) "drop" and b) "through" state; c) transmission coefficient for the through and drop state with and without cross talk (Xtalk) d) Power penalty for passing through a switch versus the number of wavelengths for optimal coupling (inset figure).

[12], and thus the set optical frequencies which will be simultaneously switched by the rings. Hence entire wavelength division multiplexed (WDM) signals can be switched by a single ring.

When designing a switching element, we are interested in maximizing the output signal quality. As the element can be in two states, we must maximize the worst case signal quality among the two states. As we will see, improving the signal quality in one state generally causes the quality of the other state to decrease. Therefore, we need to find a design where a trade-off is achieved, and therefore where the two states lead to the same signal deterioration.

In order to relate the output signal power P_{out} to the input power P_{in}we model the switch using the transfer matrix method [11]. The transfer matrices relate the input and output field amplitudes through the coupling coefficients t_1, t_2 (indicated in fig 1a and 1b). They represent the part of the signal amplitude that continues to propagate on the input waveguide. When the ring is on resonance the whole signal power is coupled into the ring if $t_1 = l_r t_2$ (known as the critical coupling condition [11]), where l_r is the optical power loss in the ring. The power "dropped" on the other waveguide is related to the input power P_{in} through $P_{drop} = DP_{in}$ with D at critical coupling given with $D = \frac{l_r^{1/2}(1-{t_2}^2)}{1-{l_r}^2{t_2}^2}$. This means that when the switch is in "drop" state and at critical coupling there is no cross talk. The dependence of *D* on the coupling parameter is shown on figure 1 c) (blue line). The signal is almost entirely "dropped" through the ring when t_2 is small while the transmission is almost entirely attenuated when $t_2 \to 1$. Should we design the switch for dropping only, a value t_1 =t_2 =0 should be targeted. However, the "through" state switch configuration requires an additional aspect to be taken into account. Even when the rings are off resonance with the inputs, a small amount of signal power is still coupled to the rings and dropped to the other waveguide. When two signals are present in the switch, some of the "leaked" power from one signal transfers to the other signal as noise, called crosstalk. With this effect in mind, the power of the transiting signal in the "through" state $P_{through}$ on port *Out1* in the ideal case when $l_r \to 1$ (a realistic assumption for small rings), is found to be

$$P_{through,Out1} = \frac{8{t_2}^4 P_{in1} - 4\sqrt{2}\sqrt{P_{in1}}\sqrt{P_{in2}}{t_2}^2(1-{t_2}^4)Sin(\Delta\phi) + P_{in2}(1-{t_2}^4)^2}{1+6{t_2}^4+{t_2}^8}. \quad (1)$$

The coefficient in front of P_{in1} in the first term gives the insertion loss (the purple line on figure 1c). The second and the third term give the cross talk, which is the largest for $\Delta\phi = \phi_1 - \phi_2 = \pi/2$, where $\phi_1(\phi_2)$ is the input phase of the signal amplitude on port 1(2). Figure 1c) also plots the worst case cross-talk (the green line) and the transmitted power $P_{through}$ at maximum cross talk (the red line). From the figure is clear that the strength of the coupling determines to a large extend the transmission and cross talk through the switch. For values of t_2 close to 1 it is very sensitive and small variations in the coupling can have significant impact on the switch transmission. From figure 1 c), we can immediately see that the optimal coupling parameter $t_{2,opt}$ is the one for which the blue line crosses the red one, i.e. the worst case decrease in quality is the same for both switch states $P_{drop} = P_{through}$. Once the optimal coupling is calculated the power penalty (in dB) of the switch is calculated by $PP_{drop} = -10Log\ D(t_{2,opt})$.

To extend this result to larger WDM switches (where the loss in the ring is nontrivial), Eq (1) is modified to include l_r. Figure 1 d) shows the power penalty at optimal coupling for different number of wavelengths and the corresponding values of $t_{2,opt}$ are displayed in the inset. Increasing the number of switched wavelengths results in increased size rings, hence increased loss l_r , which causes the cross-talk to be attenuated. Hence $t_{2,opt}$ can be progressively set to a lower value. More generally, thanks to the coupling optimization, the power penalty remains below 2 dB even for a switch capable of switching 125 wavelengths.

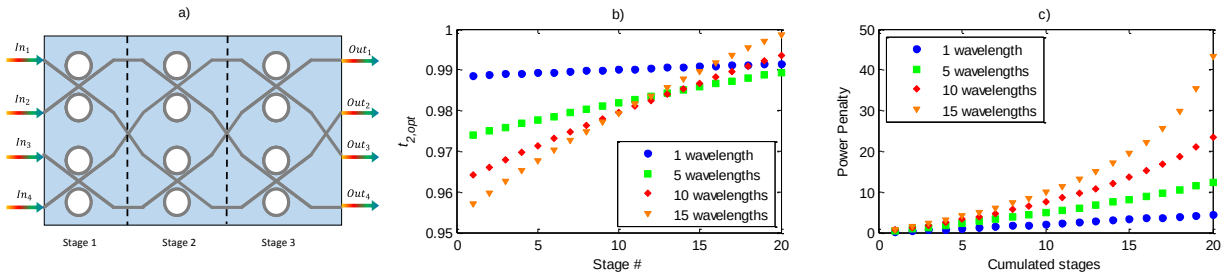

Figure 2. a) 4-by-4 multistage switch with butterfly topology b) the optimal coupling for each stage in a switch dimensioned to switch different number of wavelengths c) the power penalty vs. the number of stages.

3. MULTISTAGE SWITCH

In order to create higher radix switches, multiple 2-by-2 switches can be interconnected in stages as shown for example on figure 2 a). After each stage the signal power will be altered depending on the state of the switch. For example to reach output port *Out1* from input port *In1* the signal might be routed through three stages in drop state. To reach *Out4* from *In1* the signal can be routed via two stages in through state and one in drop state. Our objective is to minimize the worst case power penalty regardless of the states of the individual switching elements. To achieve it we optimize the coupling at each stage. For the first stage the optimal coupling is found as described in the previous section and is based on the presumption that all of the inputs have equal power. For the subsequent stages we must account the different power inputs. While the signal can interfere destructively resulting in undesired cross talk, i.e. when $\Delta\phi = \pi/2$, two signals can also interfere constructively, i.e. when $\Delta\phi = -\pi/2$. To calculate the power after passing through *S* switches, $P_{through,S}$, we have applied an iterative procedure where the input signal on port 1 for stage S $P_{in1,S}$ is taken as the worst case attenuated output signal of stage S-1, i.e. $P_{in1,S} = \min(P_{through,S-1})$. The input signal on port 2, $P_{in2,S} = \max(P_{through,S-1})$, is the one which has interfered constructively at the *S-1* previous stages. Therefore, our worst-case analysis considers the case most sensitive to crosstalk: when on input has been much attenuated and the other input has gained additive noise. Note that since we optimize the value t_2 for each stage such that through or drop signals are equilibrated, we can use $P_{through,S-1}$ or $P_{drop,S-1}$ indifferently. We replace these values in Eq. (1) (accounting for l_r) and derive the optimal coupling for stage S from solving $PP_{drop,S} = PP_{through,S}$, with $PP_{drop,S} = -10Log(D\ P_{through,S-1})$ and $PP_{through,S} = -10Log\ (P_{through,S})$, assuming $P_{in1} = P_{in2} = 1$. The derived optimal t_2 is shown on figure 2 b). As in the inset of Figure 1d, the optimal coupling is close to 1, meaning that the through state is favoured. The optimal coupling value increases with the number of stages because cross-talk accumulates and the through state gets more and more penalized. The resulting power penalty is shown on figure 2 c) for switches capable of switching 1, 5, 10 or 15 wavelengths simultaneously. For small rings (capable of switching a few wavelengths), and hence low losses, the signal can propagate 20 stages with power penalty of less than 3dB.

4. SYSTEM EVALUATION

The previous section characterizes the power penalty of a switch as a function of the number of WDM channels employed and the switch radix. Assuming a maximum amount of tolerable loss in the optical system in which these switches might be used, called the optical power budget P_{Budget}^{dB}, the maximum number of WDM channels and maximum switch radix possible can be derived. P_{Budget}^{dB} represents the ratio between the maximum total input power in the system (over all WDM channels) and the minimum power required at the photodetectors. If the total power loss of a single WDM channel is P_{Loss}^{dB}, and there are N_λ WDM channels, the following inequality must hold [14]:

$$P_{Budget}^{dB} \geq P_{Loss}^{dB} + 10log_{10}(N_\lambda) \quad (2)$$

The loss of the switch fabric P_{Loss}^{dB} includes the power penalty as calculated in section 3, the number of waveguide crossings (each incurring a 0.028 dB insertion loss [15]) and waveguide insertion loss where the length of waveguide is proportional to the diameters of all switches on the worst case optical path. We assume the switches are arranged in a Benes topology. For such a network to be rearrangeably non-blocking for *R* inputs, R/2 2-by-2 switches interconnected in $S=2\log_2 R-1$ stages are required. Figure 2a) shows an example for the Benes network for $R=4$. The exact number of waveguide crossings depends on the embedding of the Benes topology; in this work we use the same embedding as [16]. Figure 3 shows the maximum number of wavelengths which satisfy Eq. (2) for different switch power budgets. The switch power budget is agnostic of the losses in the optical system outside of the switch, the

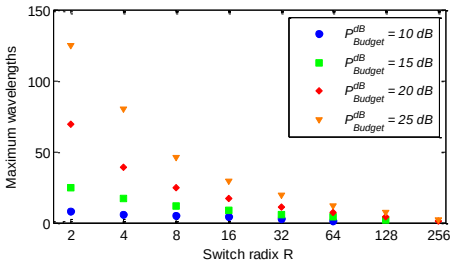

Figure 3. Maximum number of wavelengths vs. switch radix.

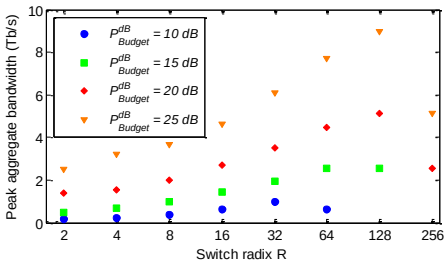

Figure 4. Peak bisectional bandwidth vs. switch radix, for different optical power budgets P^{dB}_{Budget}.

maximum allowable input power, and the photodetector sensitivity. Increasing the switch radix increases the number of stages required and hence the power penalty. In order to have loss which still satisfies Eq. (2), the supported number of wavelengths is decreased. Figure 4 shows the maximum aggregate bandwidth, or the peak bisectional bandwidth, calculated simply by multiplying the radix of the switch, the maximum number of wavelengths, and 10 Gb/s, which is the assumed data rate per wavelength channel. The last point of the curve indicates the maximum radix achievable for the given power budget. Our results show that in a system with a switch power budget of 25 dB (which corresponds to the calculations in [16]), a 128-radix transparent optical switch with up to 9 Tb/s raw bandwidth is possible.

5. CONCLUSIONS

We showed that switching element in a ring based WDM switching fabric can be optimized per stage. This permits mitigating the cross-talk and therefore attaining more scalability. Our model also illustrates that a ring based WDM switch fabric can be optimized for bandwidth, for radix, or for the product of both. When this last objective is chosen, our numerical results show that bisectional bandwidths close to 10 Tb/s is feasible for 128 radix switch with a 25dB optical power budget.

REFERENCES

[1] Y. Vlassov et al., "High-throughput silicon nanophotonic wavelength-insensitive switch for on-chip optical networks", Nature Photonics 2, 242-246 (2008).

[2] W. Zhang et al., "Broadband Silicon Photonic Packet-Switching Node for Large-Scale Computing Systems", IEEE Photonic Technology Letters, Vol. 24, No 8 , (2012).

[3] B. G. Lee et al., "High-Speed 2x2 Switch for Multiwavelength Silicon-Photonic Network-On-Chip" Journal of Lightwave Technology, Vol 27 No. 14, (2009).

[4] A. Biberman, et al.,"Broadband Photonic Electrooptic Switch for Photonic Interconnection Networks", IEEE Photonic Technology Letters, Vol. 23, No 8, (2011)

[5] N. Sherwood-Droz,et al., "Optical 4x4 hitless silicon router for optical Networks-on-Chip (NoC)", Optics Express, Vol 16, No 20, (2008)

[6] J. Kim, William J. Dally, B. Towles, A. K. Gupta, "Microarchitecture of a high radix router", ISCA'05, (2005).

[7] S. Rumley et al., "Impact of Photonic Switch Radix on Realizing Optical Interconnection Networks for Exascale Systems." Optical Interconnects, (2014).

[8] Y. Xie et al., "Crosstalk and bit error rate analysis for optical network-on-chip", DAC'10, California,USA(2010)

[9] A. Bianco, D. Cuda, R. Gaudino, G. Gavilanes, F. Neri, M. Petracca., "Scalability of Optical Interconnects Based on Microring Resonators", IEEE Photonic Technology Letters, Vol. 22, No 15 , (2010)

[10] A. Yariv, "Critical Coupling and Its Control in Optical Waveguide-Ring Resonator Systems", IEEE Photonics Tecnology Letters, Vol 14, No 4, (2002).

[11] A. Yariv, "Universal relations for coupling of optical power between microresonators and dielectric waveguides", Electronic Letters,Vol. 36, No 4, (2000).

[12] Li, G. et al, 2013. Ring Resonator Modulators in Silicon for Interchip photonic links. IEEE Journal on Selected Topics in Quantum Electronics, vol. 19, no. 6 (2013).

[13] W. Dally et al., "Principles and practices of interconnection networks." Elsevier, (2004).

[14] R. Hendry et al. "Physical layer analysis and modeling of silicon photonic WDM bus architectures." HiPEAC'14

[15] Y. Ma et al., "Ultralow loss single layer submicron silicon waveguide crossing for SOI optical interconnect." *Optics Express*, vol. 21, no. 24. November (2013).

[16] D. Nikolova et al., "High-Radix Optical Switch Based on Silicon Photonic Microring Resonators" *submitted*, ECOC (2014).